Small- and Large-Angle X-Ray Scattering Studies of Counter Ion Influence on tRNA Conformation*

Peter Wilhelm and Ingrid Pilz

Institut für Physikalische Chemie der Universität, Heinrichstraße 28, A-8010 Graz, Austria

Gábor Degovics

Institut für Röntgenfeinstrukturforschung der Österreichischen Akademie der Wissenschaften und des Forschungszentrums Graz, Steyrergasse 17, A-8010 Graz, Austria

Friedrich von der Haar

Max-Planck-Institut für Experimentelle Medizin, Abteilung Chemie, D-3400 Göttingen, Federal Republic of Germany

Z. Naturforsch. **37 c,** 1293–1296 (1982); received September 6, 1982

tRNA, conformation, small-angle X-ray scattering, large-angle X-ray scattering

The determination of cross sectional radii of gyration by small-angle X-ray scattering and comparison of large-angle scattering curves were used to study conformational changes of tRNAs depending on the concentration of mono- and divalent counter ions.

Introduction

Studies of conformational changes of tRNA depending on the ionic strength of the solution and the nature of the counter ions have become a subject of interest because of the probable role of its different conformational states for the functioning of the tRNA molecule in protein biosynthesis [1]. Results in this field obtained recently *e.g.* by pulsed nanosecond fluorometry [2] and laser light scattering [3] have caused us to use diffuse X-ray scattering techniques as a tool to obtain more information on the nature of these conformational changes. Small-angle X-ray scattering is a useful technique for studying the conformation of biopolymers in solution, and a number of studies has been carried out on tRNAs already [4–8]. Unfortunately aggregation of the tRNAs, the degree of which seems to vary with the solution conditions, may falsify determinations of parameters describing the large dimensions of the molecule (radius of gyration, maximum particle diameter). Therefore, when looking at tRNA scattering curves we have concentrated on the regions at higher angles (including the large-angle region), reflecting cross-sectional and internal structural parameters which should not be influenced by a certain degree of aggregation.

In the past few years large-angle scattering has become a useful tool for the study of the internal structure of biopolymers [9], its conformational changes [10], and comparison of similar molecules like 5 S rRNA and tRNA [11].

Experimental

Phenylalanyl-, valyl-, and isoleucyl-tRNAs were prepared from yeast as described earlier [12, 13], and dialyzed against two changes of one of the following buffers. All buffers contained 50 mM Tris-HCl pH 7.5; the additional salt concentrations were as follows:

A: 10 mM KCl, 10 mM $MgCl_2$
B: 100 mM KCl, 1 mM EDTA (to remove divalent cations)
C: 100 mM KCl, 1 mM $MgCl_2$
D: 100 mM KCl, 10 mM $MgCl_2$.

All scattering experiments were done at 17 °C. For small-angle scattering a Kratky camera with slit collimation, mounted at a Philips PW 1140 generator with a copper target (operated at 1.5 kW) was used. Experimental procedures and data evaluation have been described elsewhere [14], desmearing was done by means of indirect Fourier transformation [15].

For large-angle scattering measurements a Kratky cone camera [16] was used, smoothing and desmearing was performed by an iterative method [17] modified by P. Zipper (unpublished). The cone camera was mounted at a high energy RIGAKU DENKI RU 500 VS with rotating anode (30 kW) [18].

The scattering curves were recorded in the range $h = 0.1 - 6.9\ \mathrm{nm}^{-1}$ with the slit camera and from $h = 1.4$ to $12.0\ \mathrm{nm}^{-1}$ with the cone camera; $h = (4\pi \sin\theta)/\lambda$, 2θ = scattering angle, λ = wavelength of the CuKα line.

Molecular parameters were determined from the distance distribution function $p(r)$ (radius of gyration, maximum particle diameter) [15] and the

* Dedicated to Prof. O. Kratky on the occasion of his 80th birthday.

0341-0382/82/0300-0000 $ 01.30/0

cross-section Guinier plots (radii of gyration of the cross-section) [14], respectively.

Due to the limited available amounts of highly purified material $tRNA^{Ile}$ was investigated under two different solution conditions (A and C) only.

Results and Discussion

Under standard conditions (buffer C: 100 mM K^+, 1 mM Mg^{2+}) no significant differences between the scattering curves of the three tRNAs investigated ($tRNA^{Phe}$, $tRNA^{Val}$, $tRNA^{Ile}$) could be observed, except some minor differences in the shape of the subsidiary maximum. The curves presented in Fig. 1 a were recorded with the slit camera; they are extrapolated to zero concentration and desmeared by indirect Fourier transformation [15]. Fig. 1 b shows the distance distribution functions $p(r)$, calculated from the scattering curves. Minor differences appear only in the ranges $r = 2 - 3$ nm and $r > 6$ nm. The molecular parameters describing the large dimensions of the molecules (radius of gyration, maximum diameter) as well as the radii of gyration of the cross-sections are the same within the error limits (*cf.* Table). From the Guinier plot of the cross-section factor [14] for tRNA two different radii of gyration of the cross-section, R_{c1} and R_{c2} (Fig. 2 and Table), can be obtained probably due to two different cross-sections of the L-shaped tertiary structure of the molecule [19]. Therefore, our data suggest a very similar threedimensional structure of these three tRNA species.

If the Mg^{2+} concentration is raised to 10 mM and the K^+ concentration left at 100 mM (buffer D) the molecules tend to aggregation (striking increase of maximum dimensions, especially with $tRNA^{Phe}$), and $tRNA^{Val}$ seems to behave different from $tRNA^{Phe}$, as its cross-section decreases (R_{c1}). At reduced ionic strength (buffer A: 10 mM K^+, 10 mM Mg^{2+}) $tRNA^{Val}$ aggregates (more than $tRNA^{Phe}$ and $tRNA^{Ile}$) but the cross-sections are approximately the same as in buffer C.

The most remarkable conformational change is observed when also tigthly bound divalent cations are removed from tRNA molecules by EDTA (buffer B). Fig. 3 presents the large-angle curves of $tRNA^{Val}$ at different Mg^{2+} concentrations. While the curves are practically equal in 10 and 1 mM Mg^{2+} (differences in the height of the curves in the outer portion should not be taken too seriously, because they are very sensitive to correct background subtraction, while shapes and positions of the subsidiary maxima remain unaffected), the removal of tightly bound Mg^{2+} causes a "smearing" of the first and a shift of the second subsidiary maximum. Assuming the first subsidiary maximum at $h = 4.5\ nm^{-1}$ (Bragg distance 1.4 nm) to be associated with the distance of the double helix strains and the second (Bragg distance 0.8 nm) with the distance of

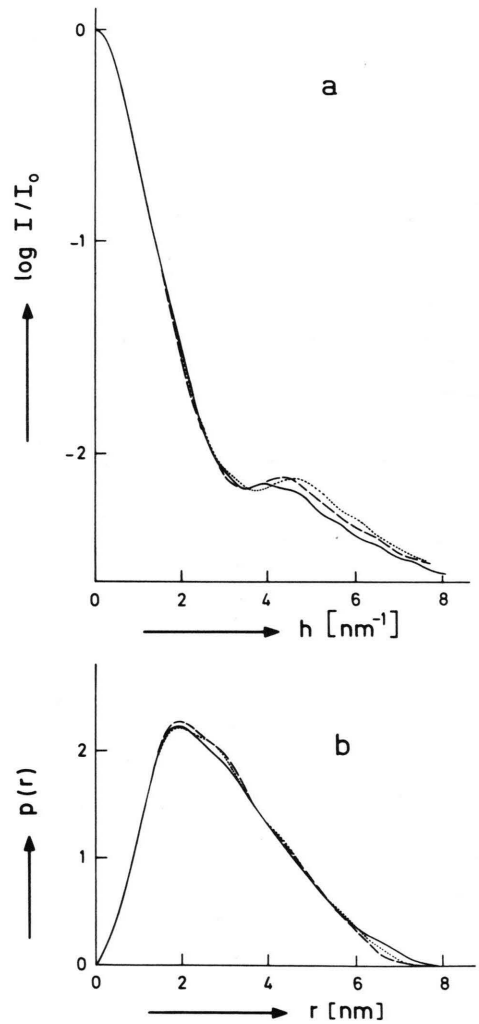

Fig. 1. a) Small-angle scattering curves of $tRNA^{Phe}$ (——), $tRNA^{Val}$ (- - -), and $tRNA^{Ile}$ (···) in buffer C (50 mM Tris-HCl pH 7.5, 100 mM KCl, 1 mM $MgCl_2$). I = scattered intensity, I_0 = scattered intensity at $h = 0$, $h = (4\pi \sin\theta)/\lambda$, 2θ = scattering angle, $\lambda = 0.154$ nm. b) Distance distribution functions $p(r)$ of $tRNA^{Phe}$ (——), $tRNA^{Val}$ (- - -), and $tRNA^{Ile}$ (···) in buffer C. r = distance, $p(r)$ in arbitrary units (all curves normalized to the same I_0).

Table. Molecular parameters obtained at different solution conditions. All buffers contain 50 mM Tris-HCl pH 7.5. R: radius of gyration, R_c: radius of gyration of the cross-section, D: maximum particle diameter.

	Buffer [mM]	R [nm]	D [nm]	R_{c1} [nm]	R_{c2} [nm]
$tRNA^{Phe}$	A (10 K^+, 10 Mg^{2+})	2.42 ± 0.05	8.4 ± 0.3	1.11 ± 0.03	0.95 ± 0.03
	B (100 K^+, no Mg^{2+})	3.00 ± 0.08	11.6 ± 0.5	1.05 ± 0.03	0.85 ± 0.03
	C (100 K^+, 1 Mg^{2+})	2.32 ± 0.05	7.8 ± 0.3	1.15 ± 0.03	0.94 ± 0.03
	D (100 K^+, 10 Mg^{2+})	3.20 ± 0.08	13.0 ± 0.5	1.14 ± 0.03	0.96 ± 0.03
$tRNA^{Val}$	A (10 K^+, 10 Mg^{2+})	2.99 ± 0.08	13.2 ± 0.5	1.15 ± 0.03	0.94 ± 0.03
	B (100 K^+, no Mg^{2+})	3.10 ± 0.08	11.5 ± 0.5	1.01 ± 0.03	0.88 ± 0.03
	C (100 K^+, 1 Mg^{2+})	2.26 ± 0.05	7.7 ± 0.3	1.15 ± 0.03	0.95 ± 0.03
	D (100 K^+, 10 Mg^{2+})	2.52 ± 0.05	10.0 ± 0.5	1.07 ± 0.03	0.92 ± 0.03
$tRNA^{Ile}$	A (10 K^+, 10 Mg^{2+})	2.50 ± 0.05	8.6 ± 0.3	1.10 ± 0.03	0.96 ± 0.03
	C (100 K^+, 1 Mg^{2+})	2.30 ± 0.05	7.5 ± 0.3	1.14 ± 0.03	0.97 ± 0.03

the phosphate groups within the same strain [4], these results may reflect a partial disorder of the ribose phosphate backbone upon removal of Mg^{2+} [20]. These changes, observed both with $tRNA^{Phe}$ and $tRNA^{Val}$, are also expressed in a decrease of the two cross-sections of 6–8% (Fig. 2 and Table).

Small conformational changes, occurring only to a certain percentage of the molecules (equilibrium between two or even more conformational states), generally cannot be detected unequivocally by scattering methods. But we feel that the results presented here strongly suggest conformational changes

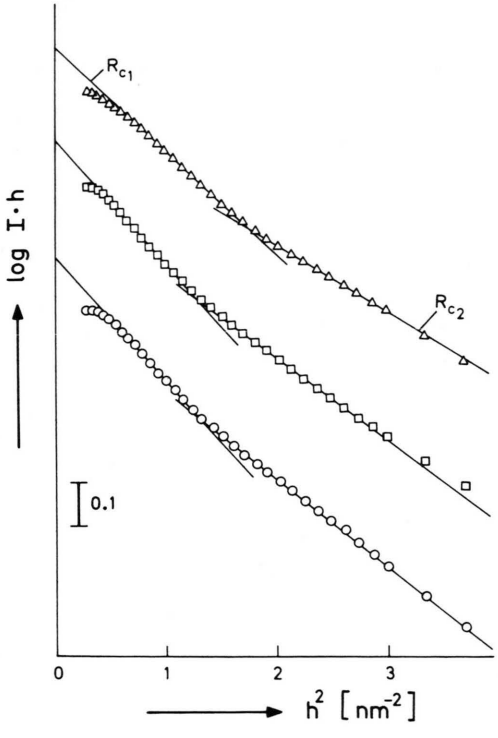

Fig. 2. Cross section Guinier plots of $tRNA^{Phe}$ at different Mg^{2+} concentrations: buffer D, 10 mM (○), buffer C, 1 mM (□), buffer B, no Mg^{2+} (△). R_c: radius of gyration of the cross section (*cf.* Table).

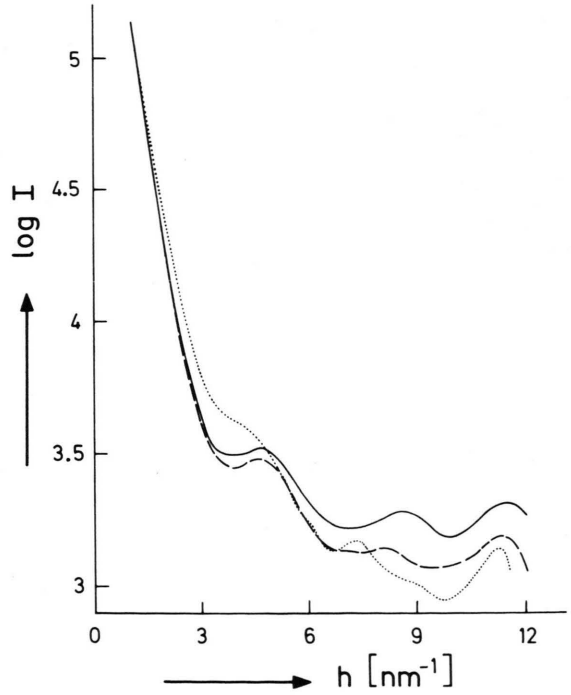

Fig. 3. Large-angle scattering curves of $tRNA^{Val}$ at different Mg^{2+} concentrations: buffer D, 10 mM (——), buffer C, 1 mM (- - -), buffer B, no Mg^{2+} (···). I in arbitrary units.

of the tRNA to be detected by scattering methods under rather extreme solution conditions (very high and very low ionic strength, removal of tightly bound divalent cations), which – in combination with the results of other methods – may help understanding the intricate functioning mechanism of this RNA species.

Thus, we hope that this investigation of three different tRNAs under varying (and somehow arbitrarily chosen) solution conditions, in addition to the above mentioned comparative study of $tRNA^{Phe}$ and 5S rRNA [11] has demonstrated the value of large-angle scattering methods for the study of conformational changes of biological macromolecules. Distinction between aggregation and conformational changes will be facilitated and comparison of structurally related biomolecules more effective, and so more experimental and methodical work in this field may be stimulated.

Acknowledgement

This work was generously supported by "Österreichischer Fonds zur Förderung der wissenschaftlichen Forschung".

[1] C. G. Kurland, R. Rigler, and C. Blomberg, Proc. Nat. Acad. Sci. USA **72,** 4248–4251 (1975).
[2] M. Ehrenberg, R. Rigler, and W. Wintermeyer, Biochemistry **18,** 4588–4599 (1979).
[3] K. W. Rhee, R. O. Potts, C.-C. Wang, M. J. Fournier, and N. C. Ford, Nucl. Acids Res. **9,** 2411–2420 (1981).
[4] J. A. Lake and W. W. Beeman, J. Mol. Biol. **31,** 115–125 (1968).
[5] I. Pilz, O. Kratky, F. Cramer, F. von der Haar, and E. Schlimme, Eur. J. Biochem. **15,** 401–409 (1970).
[6] I. Pilz, O. Kratky, F. von der Haar, and F. Cramer, Eur. J. Biochem. **18,** 436–441 (1971).
[7] J. Ninio, V. Luzzati, and M. Yaniv, J. Mol. Biol. **71,** 217–229 (1972).
[8] L. Nilsson, R. Rigler, and P. Laggner, Proc. Nat. Acad. Sci. USA, in press.
[9] J. J. Müller, H. Welfle, G. Damaschun, and H. Bielka, Biochim. Biophys. Acta **654,** 156–165 (1981).
[10] B. A. Fedorov and A. I. Denesyuk, J. Appl. Cryst. **11,** 473–477 (1978).
[11] J. J. Müller, G. Damaschun, P. Wilhelm, H. Welfle, and I. Pilz, Int. J. Biol. Macromol. **4,** 289–296 (1982).
[12] D. Schneider, R. Solfert, and F. von der Haar, Hoppe-Seyler's Z. Physiol. Chem. **353,** 1330–1336 (1972).
[13] F. von der Haar and F. Cramer, Biochemistry **17,** 3139–3145 (1978).
[14] O. Kratky, Progr. Biophys. **13,** 105–173 (1963).
[15] O. Glatter, J. Appl. Cryst. **10,** 415–421 (1977).
[16] O. Kratky, H. Stabinger, E. Wrentschur, and P. Zipper, Acta Phys. Austr. **44,** 173–189 (1976).
[17] O. Glatter, J. Appl. Cryst. **7,** 147–153 (1974).
[18] A. Jánosi and G. Degovics, Rep. Inst. Röntgenfeinstrukturforschung, Forschungszentrum Graz (1976).
[19] J. L. Sussmann, S. R. Holbrook, R. W. Warrant, G. M. Church, and S. H. Kim, J. Mol. Biol. **123,** 607–630 (1978).
[20] M. C. Chen, R. Giegé, R. C. Lord, and A. Rich, Biochemistry **14,** 4385–4391 (1975).